EUROPEAN FUSION DEVELOPMENT AGREEMENT

EFDA–JET–CP(07)03/30

A.V. Chankin, D.P. Coster, G. Corrigan, S.K. Erents, W. Fundamenski,
A. Kallenbach, K. Lackner, J. Neuhauser, R. Pitts, the ASDEX Upgrade Team
and JET EFDA contributors

Mechanisms Affecting Radial Electric Field in the Tokamak SOL

Mechanisms Affecting Radial Electric Field in the Tokamak SOL

A.V. Chankin[1], D.P. Coster[1], G. Corrigan[2], S.K. Erents[2], W. Fundamenski[2],
A. Kallenbach[1], K. Lackner[1], J. Neuhauser[1], R. Pitts[3],
the ASDEX Upgrade Team and JET EFDA contributors*

Preprint of Paper to be submitted for publication in Proceedings of the
34th EPS Conference on Plasma Physics,
(Warsaw, Poland 2nd - 6th July 2007)

INTRODUCTION

The radial electric field (E_r) is an important parameter of the Scrape-Off Layer (SOL). Via poloidal E×B drift, it directly influences poloidal motion of main ions and impurities, contributes to the parallel ion Pfirsch-Schlüter flow and toroidal momentum in the SOL, and affects asymmetries between outer and inner divertors. The magnitude of E_r in the SOL, at the same time, is a good indication of perpendicular and parallel transport processes in the SOL and divertor, including the formation of the Debye sheath at the targets [1].

A recent study revealed a large discrepancy between Er values in the SOL obtained from the experiment and simulated by 2D fluid codes [2]. SOLPS code simulations of ASDEX Upgrade (AUG) plasmas, as well as EDGE2D simulations of JET plasmas, underestimate E_r values obtained in the experiment. The ratio $-eE_r/\nabla T_e$, where both parameters are evaluated at the outer midplane, was found to be in the range 1.5 – 3 in the experiment, but < 1 in the codes. The codes also underestimate measured parallel ion SOL flows in AUG and JET. It was suggested in [2] that the E_r and flow discrepancies between the codes and experiment can be related to each other and are caused by non-local kinetic effects of parallel electron transport, including a possible impact of supra-thermal electrons on the Debye sheath formation.

The present work is aimed at establishing key mechanisms contributing to the Er formation in the SOL as seen in the present-day 2D fluid codes. The codes simulate experimental conditions using known processes of neutrals and impurities behaviour, as well as plasma motion including classical drifts. Perpendicular plasma transport, however, is described by ad-hoc transport coefficients. Fluctuations of plasma parameters existing in real turbulent plasmas are therefore ignored. Also ignored are kinetic effects in the plasma transport, as pointed out above. The codes can therefore predict some 'basic' E_r profiles; discrepancies with the experiment should then be indicative of the role of unaccounted effects.

1. EDGE2D CODE MODELLING

Basic modelling set-up for the coupled EDGE2D-Nimbus (the latter being the Monte Carlo code for neutrals) code runs simulating JET plasmas is described in [3] (Pulse No: 56723). Compared to original cases, the numerical grid was extended to include 16 rings in both core and SOL, and 8 – in the private region. Drifts were switched on everywhere across the grid, and the outer midplane separatrix density ns was kept constant by using gas puff and recycling control. Simulations were done at various ns and input power levels, in order to establish the most basic features of the Er formation in the SOL. Code results for the low density Ohmic JET shot in normal B_t configuration (ion ∇B drift towards the divertor) matching fairly well both upstream (from the divertor, along field lines) and target n_e and T_e profiles of the JET Pulse No: 56723 are presented in Fig. 1. Except for very low density cases, the simulated target T_e profile doesn't usually show a clear peak near the strike point (the same applies to SOLPS cases modelling AUG plasmas [2]). This leads to fairly flat outer target and outer midplane V_p profiles across most of the SOL, as can be seen from Fig. 1(a),

and implying a rather small radial electric field $E_r \equiv -\nabla_r V_p$. The connection between the target plasma potential and T_e is mainly determined by the Debye sheath drop $\sim 3T_e/e$, but is also affected by the current density to the target (due mainly to the thermoelectric current). The target potential propagates along the field lines to the outer midplane. However, three extra contributions accumulated along field lines arise. They follow from the parallel force balance equation for electrons (coefficient 0.71 is correct for singly charged ions) [4]:

$$E_{||} = -0.71\nabla_{||}T_e/e - \nabla_{||}p_e/en_e + j_{||}/s_{||} \quad (1)$$

Profile effects of $\nabla_{||}T_e$ and $\nabla_{||}p_e/n_e$ terms in the cases with not too low separatrix densities tend to compensate for each other, resulting in flat outer midplane V_p profiles. The ratio $-eE_r/\nabla T_e$ at the outer midplane consequently is quite low, around zero. Flatness of target T_e profiles and a small role played by the friction force lead to low upstream E_r in almost all cases (except for very low density ones, see next). A drop in the integrated $\nabla_{||}p_e/n_e$ term near the separatrix is related to the rise of the strike point p_e caused by ionization of neutrals and supported by high parallel electron heat conduction (far away from the strike point, the $\nabla_{||}p_e/en_e$ term increases upstream V_p due to the usual pressure drop towards the target).

In order to obtain positive upstream E_r, an Ohmic case with even lower separatrix density, *ns* 10^{18} m^{-3}, was run (the same can also be achieved by increasing input power for a given density). The results are presented in Fig.2. The peaked outer target T_e profile now ensures positive E_r throughout most of the SOL. The upstream E_r rise near the separatrix, however, is limited, and doesn't reflect the full extent of the Er rise near the target. The main reason for this is the large p_e increase near the strike point, sufficient to force parallel plasma flow away from the target in the divertor ('flow reversal', see e.g. [5]). The total plasma pressure including kinetic ($m_i V_i^2$) and viscous parts, is also larger at the target than upstream. Reversal of the sign of the integrated $\nabla_{||}p_e/n_e$ term approaching the separatrix reduces the upstream V_p compared to its value at the target thereby limiting the E_r rise. The outer *midplane* E_r is < outer *target* E_r near the separatrix (except for the innermost point, see Fig.3). The ratio $-eE_r/\nabla T_e$ at the outer midplane is ≈ 1 for most of the SOL, but drops towards the separatrix.

SUMMARY

Fairly flat target T_e profiles obtained in the codes (as opposed to more peaked profiles observed in experiment, for matched upstream profiles) result in low simulated outer midplane E_r values, due mainly to the flatness of the profiles of Debye sheath drops near the target. Contributions to the outer midplane E_r from the radial profiles of the $\nabla_{||}T_e$ and $\nabla_{||}p_e/n_e$ terms in the cases with not too low plasma densities largely compensate for each other, while the friction force plays a relatively minor role. Good correlation between radial profiles of the plasma potential difference ($V_{p,midplane} - V_{p,target}$) and the integrated $\nabla_{||}p_e/n_e$ term is found in all cases, regardless of the density and input power levels, or B_t direction. Positive E_r can be obtained by a large reduction in the SOL plasma density

(or increase in the input power) that creates peaked target T_e profiles. The E_r rise, however, is limited by the increase in the relative importance of the $\nabla_{\|}p_e/n_e$ term owing to the electron pressure rise near the strike point, which also forces the 'flow reversal' in the divertor just outside of the separatrix. The discrepancy between experimental $-eE_r/\nabla Te$ ratios obtained from Langmuir probe measurements (~ 1.5 – 3) and simulated values (< 1) indicate the presence of some additional mechanisms not covered by standard fluid codes.

REFERENCES

[1]. Stangeby P.C, in *The Boundary of Magnetic Fusion Devices*, IOP Publishing, Bristol (2000).

[2]. Chankin A.V, Coster D P, Asakura N, et al., Nucl. Fusion **47** (2007) 479.

[3]. Erents S.K, Pitts R A, Fundamenski W, et al., Plasma Phys. Control. Fusion **46** (2004) 1757.

[4]. Braginskii S.I, in *Reviews of Plasma Physics*, edited by M.A.Leontovich (Consultants Bureau, New York, 1965), Vol. 1, p. 205.

[5]. LaBombard B, et al., J.Nucl. Mater. **241-243** (1997) 149.

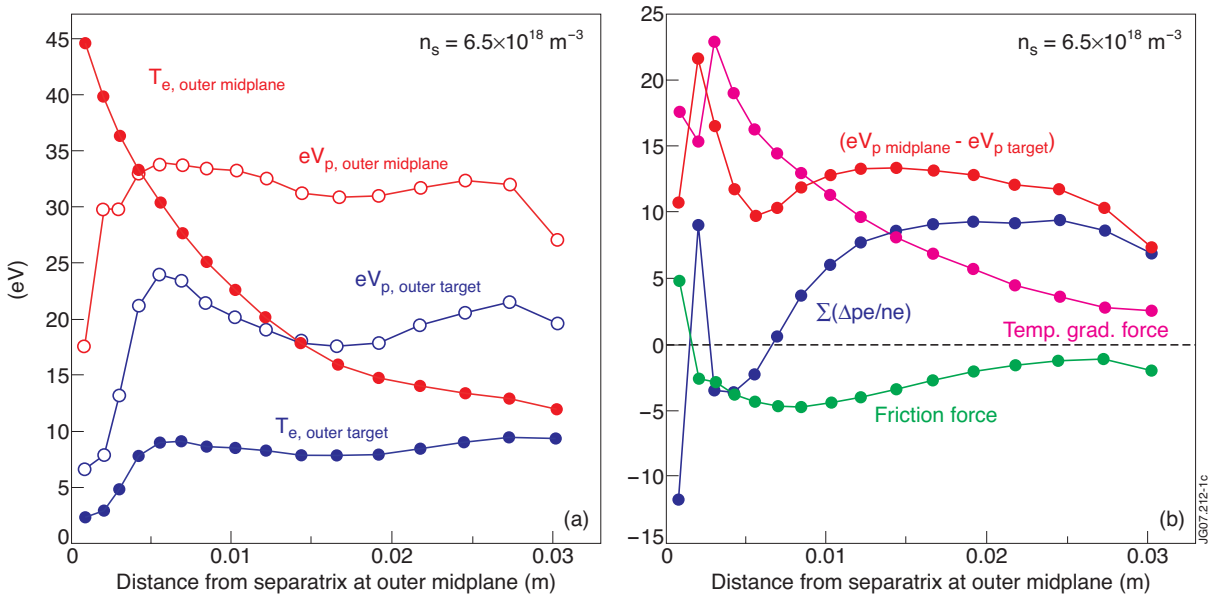

Figure 1: T_e and plasma potential V_p (multiplied by elementary change e) at the outer midplane, T_e and eV_p at the outer target (a); the difference between outer midplane and outer target eV_p, and its contributions: integrated friction force $ej_{\|}/\sigma_{\|}$, integrated temperature gradient force $\approx -0.71 - V_{\|}T_e$, and integrated pressure gradient force - $\nabla_{\|}p_e/n_e$ (marked as $\Sigma(\Delta p_e/n_e)$ (b), for Ohmic JET case with $n_s = 6.5\times10^{18}m^{-3}$. The distance from the separatrix is mapped to the outer midplane position.

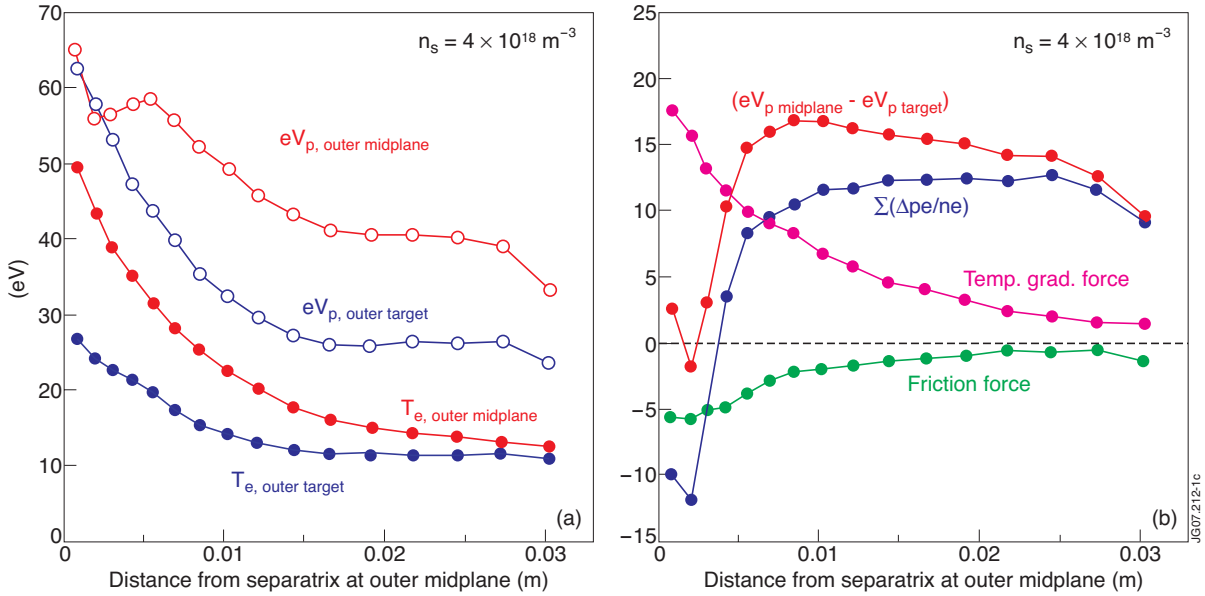

Figure 2: Same data as shown in Fig.1, but for the lower density Ohmic case, with $n_s = 4{\times}10^{18}m^{-3}$.

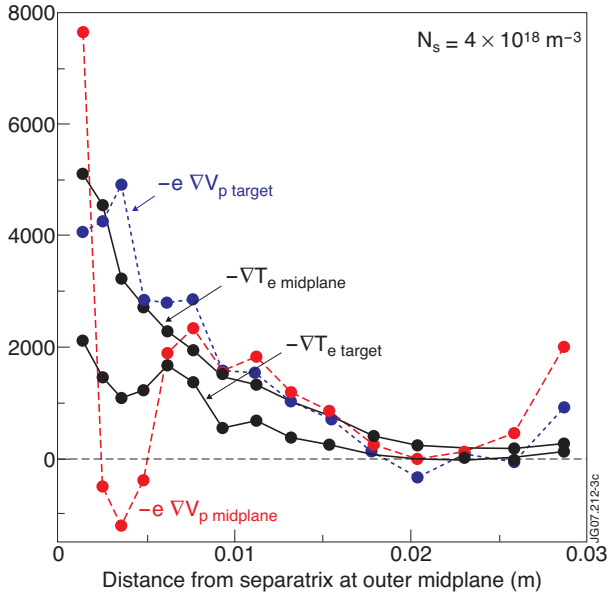

Figure 3: eE_r at outer target and midplane, $-\nabla T_e$ at outer target and midplane, for the case shown in Figure 2.